

The nonflow issue in connecting anisotropy measurements to hydrodynamics in relativistic heavy-ion collisions

Fuqiang Wang^{1,*}

¹*Department of Physics and Astronomy, Purdue University, West Lafayette, IN 47907*

Hydrodynamics can describe majority of the measured azimuthal anisotropies in relativistic heavy-ion collisions. Many of the anisotropy measurements are contaminated by nonflow correlations (i.e., those unrelated to global event-wise correlations). Those nonflow contamination can cause incorrectness or compromise the accuracy of the physics extracted from data-hydrodynamics comparison, particularly when one relies on subtle difference in the measurements. In the recent preprint by STAR (arXiv:2401.06625) extracting the Uranium nucleus deformation parameter, nonflow contamination is assessed by subevents in the limited STAR acceptance. In this note, we demonstrate that such assessment is inadequate and illustrate how large an effect nonflow can cause by using the HIJING model, in which all correlations are nonflow and non-hydrodynamic. We thereby conclude that the extracted Uranium deformation parameter is premature and emphasize the importance of an earnest assessment of or correction for nonflow contamination, not only for this STAR analysis but more generally for studies relying on comparing anisotropy measurements to hydrodynamic calculations.

1. INTRODUCTION

Anisotropic flow is a hallmark of heavy-ion (nucleus-nucleus) collisions. It arises from interactions converting the anisotropy in configuration space of a nucleus-nucleus collision into momentum space [1]. The configuration space anisotropy is prominent in non-central collisions where the overlap interaction zone is of an almond shape. The anisotropy is nonzero even in central head-on collisions because of position fluctuations of nucleons in the colliding nuclei, giving rise to finite eccentricities [2]. Because of the same reason, nonzero anisotropy can also emerge in small-system collisions, such as proton-proton and proton-nucleus collisions [3, 4].

The interactions in the system created in relativistic heavy-ion collisions, presumably the quark-gluon plasma (QGP), are governed by quantum chromodynamics (QCD). How exactly those interactions convert the initial-state geometry anisotropy into final-state momentum anisotropy is not well settled. It is generally believed that ultra-strong interactions are required to produce the observed large anisotropy (or flow) in midcentral to central heavy-ion collisions, and the QGP created in those collisions is a nearly perfect fluid [5] and can be well described by viscous hydrodynamics [6]. In peripheral heavy-ion collisions and small-system collisions, the interactions may not be strong enough where hydrodynamics would be applicable and the escape mechanism may be at work [7–10].

Interactions also generate transverse momentum, absent in the initial state. Event-by-event correlations between transverse momentum and momentum anisotropy naturally emerge. For instance, in head-on collisions of spherical nuclei, a fluctuated smaller interaction zone result in stronger interactions causing positive correlations

between elliptic anisotropy (v_2) and event-wise mean transverse momentum ($[p_T]$). An interesting case is deformed nuclei like the Uranium (U): in central U+U collisions, tip-tip configuration yields a smaller and more spherical collision zone, hence larger $[p_T]$ and weaker v_2 , whereas body-body configuration gives a larger and less spherical collision zone, hence smaller $[p_T]$ and stronger v_2 ; a v_2 - p_T anti-correlation results [11, 12].

Because anisotropic flow is a result of interactions from an anisotropic initial geometry, studies of anisotropic flow can reveal important physics about the interactions and the initial geometry. Two types of studies can be taken: (1) with colliding nuclei of well measured density distributions, one may gain information about the created QGP, such as its shear viscosity to entropy density ratio, via its hydrodynamic responses [13]; and (2) with well-controlled hydrodynamic responses, one may probe structures of the colliding nuclei and thereby the physics governing those structures [12, 14]. Because the conversion from initial-state geometry anisotropy to final-state momentum anisotropy is dependent of the system evolution, significant uncertainties are inevitable [15, 16].

For studies of type (2), an effective strategy is to utilize a pair of nuclei close in mass number with yet appreciable difference in their density distributions (nuclear structure). One example is the isobar $^{96}_{44}\text{Ru}+^{96}_{44}\text{Ru}$ and $^{96}_{40}\text{Zr}+^{96}_{40}\text{Zr}$ collisions, conducted in 2018 at the Relativistic Heavy-Ion Collider (RHIC) to search for the chiral magnetic effect [17–21]. Density functional theory calculations revealed differences in the nuclear structures and neutron skins of the Ru and Zr nuclei, predicting significant differences in the final-state multiplicities and anisotropic flows between the isobar collisions [14, 22, 23], later confirmed by experiment [21].

However, there is an important complication with anisotropic flow measurements (and similarly other correlation measurements). Flow anisotropies are often mea-

* fqwang@purdue.edu

sured by two-particle correlations via

$$\langle V_n \rangle = \langle \cos n(\phi_1 - \phi_2) \rangle, \quad (1)$$

where ϕ_1 and ϕ_2 are the azimuthal angles of two particles of interest (POI), and n is the harmonic order (for instances, $n = 2$ for elliptic flow and $n = 3$ for triangular flow). The goal is to measure the collective anisotropic flow v_n arising from global event-wise correlations to the azimuthal harmonic planes (ψ_n), $dN/d\phi \propto 1 + \sum_{n=1} 2v_n \cos n(\phi - \psi_n)$ [24]. In the ideal case where collective flow is the only physics, then $V_n = v_n^2$. However, there exist other physics correlations, such as those from resonance decays, jet-like correlations [25, 26], and initial-state gluon correlations [27], independent of the global event-wise correlations. Those “genuine” correlations are termed nonflow and contaminate the measured $\langle V_2 \rangle$ of Eq. (1) [28–31].

Resonance decays and intrajet correlations usually result in particles close in pseudorapidity (η) and azimuthal angle (dubbed near-side correlations). Their contamination can be reduced by applying an η -gap between the two POIs or by requiring them to come from phase spaces (subevents) separated in η [32]. Interjet correlations, or generally momentum conservation effects, usually yield particles back-to-back in azimuth but not locally confined in η (dubbed away-side correlations). These nonflow contamination are difficult to remove, and one may resort to model studies or data-driven fitting techniques in 2-dimensional pseudorapidity and azimuthal differences ($\Delta\eta \equiv \eta_1 - \eta_2$, $\Delta\phi \equiv \phi_1 - \phi_2$) of two-particle correlations [33, 34]. Because resonance abundances are expected to scale with the final-state multiplicity, nonflow contribution to $\langle V_2 \rangle$ by Eq. (1) is approximately proportional to inverse multiplicity. Jet correlations and nuclear effects like jet quenching and baryon-over-meson enhancement may cause nonflow to deviate from such a simple multiplicity scaling. In general, nonflow contamination is severe in peripheral collisions and become less so towards more central collisions. However, since the collective flow contribution also decreases with increasing centrality because of the more spherical collision zone, nonflow contamination in central collisions can still be appreciable, whereas it is generally the smallest in mid-central collisions. Experimental data indicate that nonflow contributions can be as large as a few tens of percents in central heavy-ion collisions [33–36].

Despite of a minor contribution to the measured V_n anisotropies, the effect of nonflow can be significant when one is probing small differences in the physics relying on delicate cancellation of final-state effects. For example, relatively large differences in elliptic flow and triangular flow have been observed between central isobar collisions, suggesting significant differences in the deformations of the isobar nuclei [21]. It is attempting to extract those deformations directly from their ratio measurements between central isobar collisions, ignoring nonflow contamination, as was done in Ref. [37]. However, nonflow contamination is important considering the fact that the

Ru+Ru/Zr+Zr ratio of $\langle V_2 \rangle$ is larger than unity whereas the ratio of nonflow is smaller than unity (because of the larger multiplicity in Ru+Ru than in Zr+Zr collisions). The measured isobar ratio of $\sqrt{\langle V_2 \rangle}$ is 1.025 for full-event and 1.028 for subevent method in the top 0-5% central isobar collisions [21]. Nonflow estimates by $(\Delta\eta, \Delta\phi)$ fit [33, 34] indicate $\sim 37\%$ and $\sim 30\%$ nonflow contamination in the measured $\langle V_2 \rangle$ by the full-event and subevent methods, respectively (those nonflow contamination are larger than that in central Au+Au collisions because the multiplicities are correspondingly smaller). As a result, the isobar ratio of the “genuine” v_2 is 1.046, significantly larger than the measured ratios of $\sqrt{\langle V_2 \rangle}$ [33, 34]. This would imply that the quadruple deformation difference between Ru and Zr nuclei could be larger than extracted simply from the measured anisotropy difference in Ref. [37].

Clearly, nonflow contamination should be removed with well-controlled systematic uncertainties before data can be compared to hydrodynamic model calculations to extract relevant physics quantities. The STAR experiment has recently released a preprint [38] extracting the quadruple deformation parameter β_{2U} of the U nucleus by comparing the ratios of the measured $\langle v_2^2 \rangle$, $\langle (\delta p_T)^2 \rangle$ (where $\delta p_T = [p_T] - \langle [p_T] \rangle$), and $\langle v_2^2 \delta p_T \rangle$, respectively, between two relatively close systems of U+U and Au+Au collisions to those calculated by hydrodynamic models. The nonflow contamination is assessed by the subevent method. It is known that the η -gap or subevent method can only remove part of the nonflow contamination; for example, the away-side nonflow correlations cannot be removed. It is imperative to examine the effects of remaining nonflow contamination or, more generally, non-hydrodynamic contributions to the measured quantities (e.g., jet contributions to the v_2 - p_T correlations) on the extracted physics.

To this end, we employ a non-hydrodynamic model, the HIJING event generator [39, 40] to investigate those effects. HIJING is particularly suitable for this study because it is a jet production model with nuclear jet-quenching effects and at the same time contains reasonable descriptions of particle and resonance production. Moreover, it does not have collective flow so the entire azimuthal anisotropy is nonflow; there is no question about the separation of flow and nonflow.

2. SIMULATION AND ANALYSIS

The purpose of our study is to examine quantitatively how important nonflow and non-hydrodynamic correlations are to $\langle v_2^2 \rangle$, $\langle (\delta p_T)^2 \rangle$, and v_2 - p_T correlations, but not the effects of nuclear deformation of the Uranium (U) or Gold (Au) nuclei. To illustrate the essential point of our study, we keep both the Au and U nuclei spherical. The nuclear densities are given by the Woods-Saxon distributions, $\rho \propto [1 + \exp(\frac{r-R}{a})]^{-1}$. The radius parameter R for Au is 6.38 fm and for U is 6.8 fm [41]. The surface

diffuseness parameter $a = 0.535$ fm is set to be the same for both nuclei. We expect the subtle differences in the density distributions and deformations between the two nuclei will only cause high-order effects, without affecting our main conclusions.

The default HIJING (version 1.41) is used. Jet-quenching is switched on. The impact parameter range is set to the maximum of 20 fm to ensure minimum-bias (MB) event samples. Total 3.8×10^8 MB events are simulated each for U+U collisions at 193 GeV and Au+Au collisions at 200 GeV.

The centrality percentiles are determined by the final-state charged hadron multiplicity distributions within pseudorapidity range $|\eta| < 0.5$, similar to experiment [42]; the maximum multiplicity corresponds to centrality 0% and the minimum corresponds to centrality 100%.

The azimuthal anisotropy is computed by Eq. (1) averaged over all pairs and all events [32]. It can alternatively be computed by averaging over all pairs in an event first and then over all events treating each event equal weighted. The difference is negligible. The p_T fluctuation is also computed by two-particle correlator

$$\langle(\delta p_T)^2\rangle = \langle(p_{T,1} - \langle p_T \rangle)(p_{T,2} - \langle p_T \rangle)\rangle. \quad (2)$$

The alternative calculation by averaging first within event and then over all events, $\langle[p_{T,1}p_{T,2}] - \langle p_T \rangle^2\rangle$, yields negligible difference. The v_2 - p_T correlation is obtained by computing event-wise average quantities first and then averaging over all events with equal weight, namely,

$$\langle v_2^2 \delta p_T \rangle = \langle [\cos 2(\phi_1 - \phi_2)]([p_T] - \langle p_T \rangle) \rangle, \quad (3)$$

where $[\cos 2(\phi_1 - \phi_2)]$ stands for the event-wise average of the correlator. Using three-particle cumulant to compute $\langle v_2^2 \delta p_T \rangle$ yields consistent result because the same particle used in computing $[\cos 2(\phi_1 - \phi_2)]$ and $[p_T]$ does not cause self-correlations.

3. SIMULATION RESULTS

Figure 1 upper panel shows the nonflow correlations in HIJING calculated by Eq. (1) as functions of centrality from 60% to 0% in Au+Au and U+U collisions. The POIs are both taken from $|\eta| < 1$ (full-event method). The nonflow in U+U is lower than that in Au+Au by approximately 20%, the multiplicity difference at a given centrality. In the top 0-5% centrality, the HIJING nonflow correlations are $\langle V_2 \rangle \approx 0.6 \times 10^{-4}$ in Au+Au and 0.5×10^{-4} in U+U collisions, respectively.

The lower panel of Fig. 1 shows the charged hadron multiplicity (N_{ch}) scaled nonflow correlations, $N_{\text{ch}}\langle V_2 \rangle$, for both full-event and subevent methods. The subevent method takes one POI from $-1 < \eta < -0.1$ and the other from $0.1 < \eta < 1$. The $N_{\text{ch}}\langle V_2 \rangle$ values are consistent between the two systems, indicating the same nonflow sources diluted by multiplicity. The $N_{\text{ch}}\langle V_2 \rangle$ values

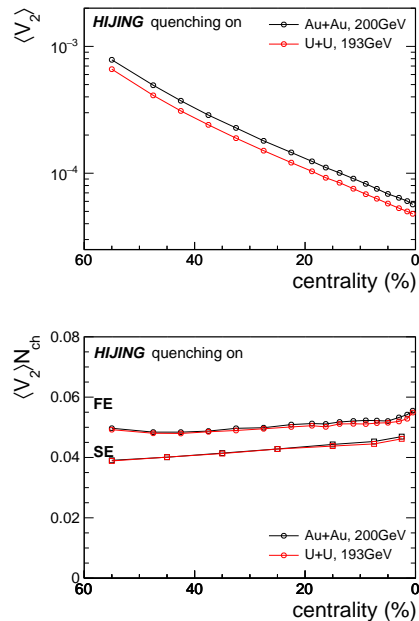


FIG. 1. HIJING nonflow $\langle V_2 \rangle$ results. (Upper) Two-particle nonflow $\langle V_2 \rangle$ of Eq. (1) as functions of increasing centrality in spherical Au+Au (black) and spherical U+U (red) collisions. Particles of interest (POI) are taken from pseudorapidity range $|\eta| < 1$, and no η -gap is applied between the two particles (full-event). (Lower) The multiplicity scaled nonflow $N_{\text{ch}}\langle V_2 \rangle$ from the full-event (FE, circles) method, as well as from the subevent (SE, squares) method where one POI is taken from $-1 < \eta < -0.1$ and the other from $0.1 < \eta < 1$.

show only a minor increase with centrality, in line with the approximate inverse multiplicity scaling of nonflow. The minor increase may be attributed to final-state nuclear effects like jet-quenching and enhanced heavy resonance production. The reduction in nonflow from the full-event to subevent method is small, only 12% in the most central collisions. This implies that the away-side correlations make a large contribution to the overall nonflow, the near-side correlations are broad and the η -gap applied by the subevent method removes only part of the near-side nonflow, or likely both.

Figure 2 shows the p_T fluctuations calculated by Eq. (2) with the full-event method in Au+Au and U+U collisions as functions of centrality. The $\langle(\delta p_T)^2\rangle$ values are approximately 20% smaller in U+U than in Au+Au collisions, similar to the $\langle V_2 \rangle$ results in Fig. 1. This is because both quantities are essentially two-particle correlation measures and are diluted similarly by multiplicity. The lower panel of Fig. 2 shows the multiplicity scaled p_T fluctuations, $N_{\text{ch}}\langle(\delta p_T)^2\rangle$. Indeed, the $N_{\text{ch}}\langle(\delta p_T)^2\rangle$ values equal between Au+Au and U+U collisions at a given centrality. The $N_{\text{ch}}\langle(\delta p_T)^2\rangle$ value exhibits a modest decrease with increasing centrality.

Figure 3 left panel shows the event-by-event correlations between $\langle V_2 \rangle$ and $\delta p_T / \langle p_T \rangle$ calculated by HIJING

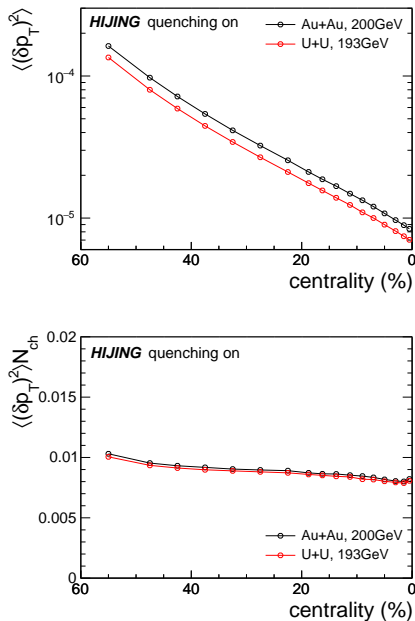


FIG. 2. HIJING p_T correlation $\langle(\delta p_T)^2\rangle$ results. Event-wise p_T fluctuations as functions of centrality in spherical Au+Au (black) and spherical U+U (red) collisions. The POIs are taken from pseudorapidity range $|\eta| < 1$, and no η -gap is applied between the two particles (full-event).

in the top 0-0.5% centrality for Au+Au and U+U collisions. The correlations are positive and the correlation strengths appear to be similar in terms of the slope of $\langle V_2 \rangle$ vs. $\delta p_T / \langle p_T \rangle$. This can be understood by minijets which contribute to both nonflow and p_T fluctuations and the physics is no different between Au+Au and U+U. The overall value of $\langle V_2 \rangle$ is smaller in U+U than in Au+Au because of the multiplicity difference (see Fig. 1), so the $\langle v_2^2 \delta p_T \rangle$ value is smaller.

The center panel of Fig. 3 shows the v_2 - p_T correlation quantity $\langle v_2^2 \delta p_T \rangle$ in Au+Au and U+U collisions as functions of centrality. Similar to $\langle V_2 \rangle$ and $\langle(\delta p_T)^2\rangle$, the U+U system shows a smaller correlation magnitude than the Au+Au system, by approximately 30-40%. This is in line with the smaller magnitudes of $\langle V_2 \rangle$ and $\langle(\delta p_T)^2\rangle$ in U+U than in Au+Au collisions, each by approximately 20% as shown in Figs. 1 and 2, respectively. Indeed, the N_{ch}^2 scaled v_2 - p_T correlations are similar between the two systems as shown in the right panel of Fig. 3.

It is clear that $\langle V_2 \rangle$, $\langle(\delta p_T)^2\rangle$, and $\langle v_2^2 \delta p_T \rangle$ correlations are all nonzero in HIJING. These correlations are all caused by non-hydrodynamic origins because HIJING is not a hydrodynamic model. HIJING describes jet production in hadron-hadron, hadron-nucleus, and nucleus-nucleus collisions, and jet quenching by partonic energy loss in the final-state nuclear medium [39, 40]. HIJING has also reasonable descriptions of soft particle and resonance production via string fragmentation. Therefore, the $\langle V_2 \rangle$, $\langle(\delta p_T)^2\rangle$, and $\langle v_2^2 \delta p_T \rangle$ correlations observed in

HIJING presumably arise mainly from jet correlations and resonance decays.

4. IMPLICATIONS TO STAR DATA AND DISCUSSIONS

In the recent preprint [38], the STAR experiment compared ratios of correlation quantities in U+U collisions at 193 GeV over Au+Au collisions at 200 GeV to those calculated by the IP-Glasma+MUSIC hydrodynamic model [43, 44] to extract the deformation parameters of the U nucleus. From the ratio of the measured $\langle v_2^2 \rangle$, the extracted quadrupole deformation parameter is $\beta_{2U} = 0.240 \pm 0.014$; this value is, however, discounted attributing to an inadequate description of v_2 by hydrodynamics (cf Figure 3a of Ref. [38]). From the simultaneous comparisons of the measured $\langle(\delta p_T)^2\rangle$ ratio and $\langle v_2^2 \delta p_T \rangle$ ratio to hydrodynamic calculations, the quadrupole deformation and triaxiality parameters are extracted to be $\beta_{2U} = 0.297 \pm 0.013$ and $\gamma_U = 8.6^\circ \pm 4.7^\circ$, respectively. Comparing to another hydrodynamic model (trajectum [45]) leads to a value of $\beta_{2U} = 0.273 \pm 0.015$. This value is not covered by the quoted systematic uncertainty of the main β_{2U} result.

The nonflow contamination in $\langle v_2^2 \rangle$ is assessed in the STAR work [38] as follows: the $\langle v_2^2 \rangle$ is taken to be the average of the full-event measurement where POIs are taken from the STAR Time Projection Chamber (TPC) acceptance ($|\eta| < 1$) and the subevent measurement where the POIs are from separate subevents ($-1 < \eta < -0.1$ and $0.1 < \eta < 1$), and half of their difference is taken to be the systematic uncertainty. The $\langle(\delta p_T)^2\rangle$ and $\langle v_2^2 \delta p_T \rangle$ are measured similarly by full-event and subevent methods, and their systematic uncertainties are assessed in similar ways. The assessed *nonflow* systematic uncertainties are 1-2% for $\langle v_2^2 \rangle$, 1-3% for $\langle(\delta p_T)^2\rangle$, and 2-4% for $\langle v_2^2 \delta p_T \rangle$, with the corresponding *total* systematic uncertainties to be 2.5-4%, 2-5%, and 4-10%, respectively.

Figure 1 shows that $\langle V_2 \rangle = 0.6 \times 10^{-4}$ in the most central 0-5% Au+Au collisions in HIJING. This is about 12% of the measured $\langle v_2^2 \rangle = 5 \times 10^{-4}$ [38] in the same centrality range of Au+Au collisions. According to HIJING, only 12% of it (i.e., 12% of the 12% nonflow) is removed by the subevent method, as shown in the lower panel of Fig. 1. This implies that significant nonflow remains in the STAR $\langle v_2^2 \rangle$ measurement, and the nonflow uncertainty is severely underestimated in [38], possibly by an order of magnitude (a factor of 15 based on HIJING face value). Because nonflow approximately scales with the inverse multiplicity which differs by 20% between Au+Au and U+U collisions, a 12% remaining nonflow would yield a 2% effect in the ratio of $R_{v_2^2} = \langle v_2^2 \rangle_U / \langle v_2^2 \rangle_{Au}$. The real situation is worse because the v_2 in central U+U collisions is larger due to its deformity (see Figure 4a of Ref. [38]), so the nonflow contamination in central U+U is significantly smaller than in Au+Au, making the effect on the ratio $R_{v_2^2}$ much larger (this point is more quanti-

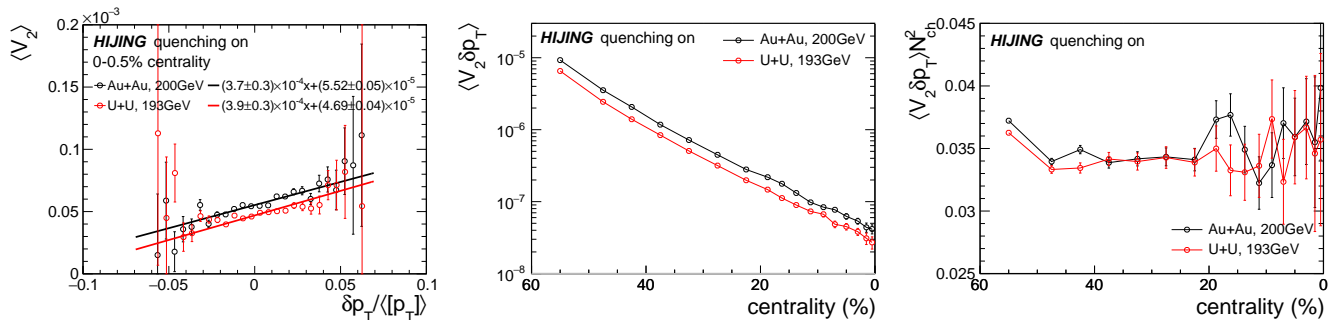


FIG. 3. HIJING v_2 - p_T correlation results. Event-by-event correlations between $\langle V_2 \rangle$ and $\delta p_T / \langle [p_T] \rangle$ in the top 0-0.5% centrality (left panel), correlation covariance $\langle v_2^2 \delta p_T \rangle$ as functions of centrality (center panel), and the multiplicity scaled $N_{ch}^2 \langle v_2^2 \delta p_T \rangle$ (right panel) in spherical Au+Au (black) and spherical U+U (red) collisions. The POIs are taken from pseudorapidity range $|\eta| < 1$, and no η -gap is applied between the two particles (full-event).

tatively presented later).

It is conceivable that non-hydrodynamic correlations in p_T - p_T and v_2 - p_T correlations cannot be completely removed by the subevent method either. Part of those non-hydrodynamic correlations are due to minijets which are wide objects comparable to the STAR TPC acceptance; furthermore, dijet correlations go far beyond the acceptance. It is reasonable to conjecture that majority of those non-hydrodynamic correlations remain in $\langle (\delta p_T)^2 \rangle$ and $\langle v_2^2 \delta p_T \rangle$, like in $\langle v_2^2 \rangle$. This implies that the uncertainties due to nonflow and non-hydrodynamic correlations could be much larger than estimated in [38], easily reaching 10% or beyond.

Since nonflow can be corrected in many analyses, including this recent STAR work [38], it should rather be treated as a systematic error and be corrected, not simply a systematic uncertainty. Earnest efforts should be spent to correct for the systematic errors and assess the systematic uncertainties on such corrections. With this in mind, we compare in Fig. 4 left panels our HIJING calculations of the quantities $\langle v_2^2 \rangle$, $\langle (\delta p_T)^2 \rangle$, and $\langle v_2^2 \delta p_T \rangle$ to those measured by STAR [38]. In the middle and right panels of Fig. 4, we illustrate how the measured U+U/Au+Au ratios of these quantities would move and how the extracted deformation parameters would change if nonflow and non-hydrodynamic effects were corrected according to HIJING.

Figure 4 left-top panel shows that the measured $\langle v_2^2 \rangle$ values in the top 0-5% centrality are approximately 5×10^{-4} for Au+Au and 8×10^{-4} for U+U. The significantly larger $\langle v_2^2 \rangle$ measured for U+U is due to the large quadrupole deformation. Thus, the HIJING nonflow contributions to $\langle v_2^2 \rangle$ would be 12% in central Au+Au and 6% in central U+U collisions. This would result in an increased $R_{v_2^2}$ by 6% in the top 0-5% centrality, in contrast to the 2% from simple multiplicity scaling aforementioned. This is illustrated in the center- and right-top panels of Fig. 4. Subtracting HIJING nonflow from data would raise the STAR data points to the red circles in the center-top panel, and the hatched area of the top 0-5%

data to the red box in the right-top panel. This is about 6 times the estimated systematic uncertainty on $\langle v_2^2 \rangle$ due to nonflow in [38]. It is not quite as large as the factor of 15 mentioned earlier, possibly implying that nonflow in HIJING is an underestimate for real data and/or the subevent method is less effective in HIJING. Indeed, the estimated nonflow in the full-event v_2^2 data is on the order of 20% in central Au+Au collisions [35].

Figure 4 left-middle panel shows that $\langle (\delta p_T)^2 \rangle$ from HIJING is also appreciable compared to the STAR data. The U+U data increase towards central collisions presumably because of its deformity. In the most central 0-5% collisions, the $\langle (\delta p_T)^2 \rangle$ value in HIJING is $\sim 20\%$ of that measured in Au+Au, while that for U+U is $\sim 10\%$. Correcting for these non-hydrodynamic effects would increase the ratio of $R_{(\delta p_T)^2} = \langle (\delta p_T)^2 \rangle_U / \langle (\delta p_T)^2 \rangle_{Au}$ by approximately 10% in the top 0-5% centrality, again several times the estimated systematic uncertainty due to nonflow in [38]. This is illustrated in the center- and right-middle panels of Fig. 4, similarly to the corresponding top panels.

Figure 4 left-bottom panel shows that the $\langle v_2^2 \delta p_T \rangle$ correlations in HIJING are strong in the 60-50% centrality range and rapidly decrease towards central collisions. The decrease in the measured data is not as rapid. For the top 0-5% central Au+Au collisions, $\langle v_2^2 \delta p_T \rangle$ from HIJING is approximately 5×10^{-8} , about 10% of that measured in data. In central U+U collisions, the measured $\langle v_2^2 \delta p_T \rangle$ correlations become significantly negative, presumably because of hydrodynamic responses to the large deformation of the U nucleus. The $\langle v_2^2 \delta p_T \rangle$ correlations from HIJING remain positive in the top 0-5% central U+U collisions, approximately 3.5×10^{-8} . This is about 6% of the magnitude of the measured negative v_2 - p_T correlations in 0-5% central U+U collisions. The positive correlations in HIJING likely arise from fluctuations in resonance p_T and jet production. For the former, the larger the resonance p_T , the smaller the decay opening angle, and thus the larger the nonflow V_2 . For the latter, the more the jet production, the larger the $[p_T]$ and the larger

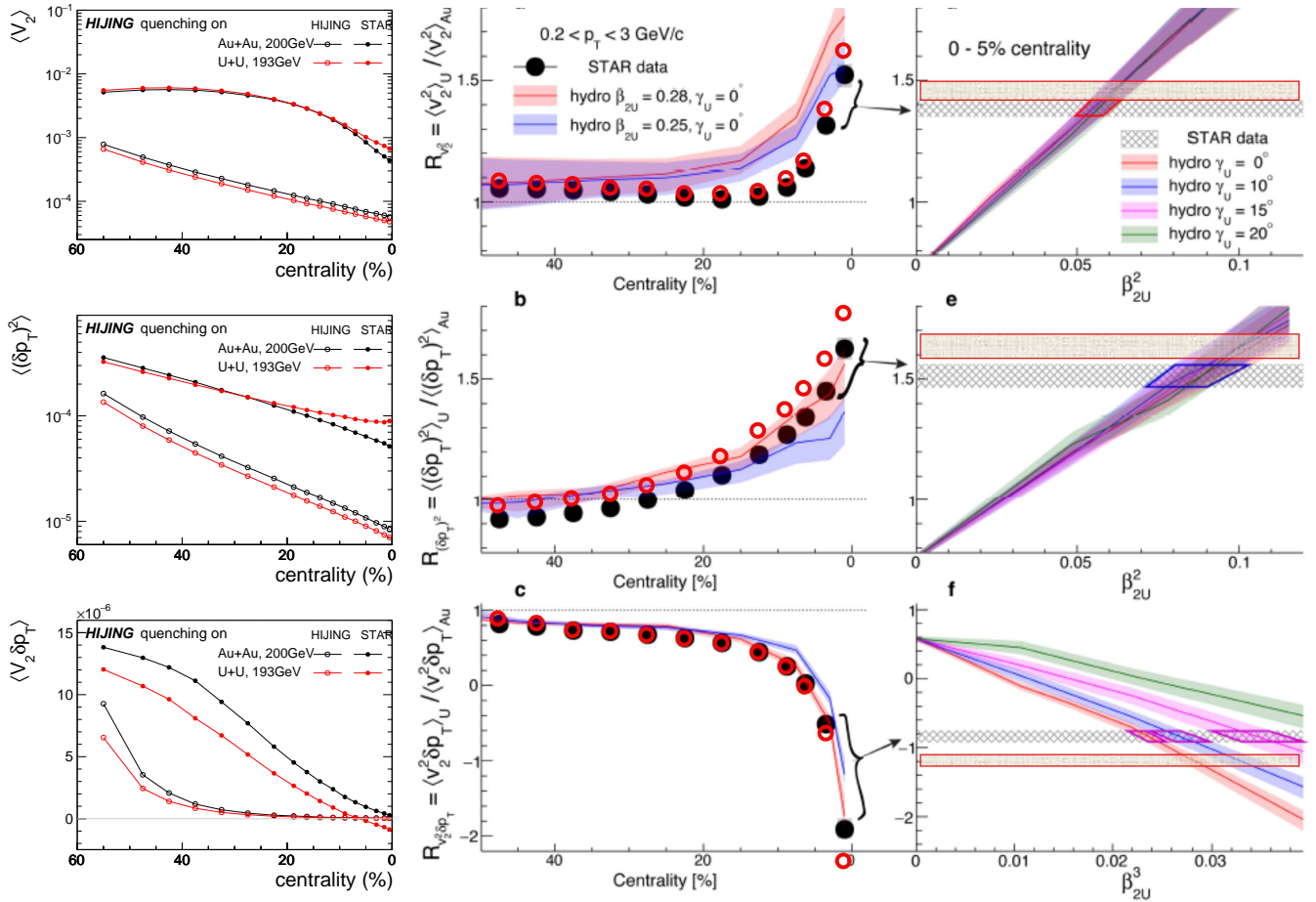


FIG. 4. Effects of non-hydrodynamic correlations on STAR data. (Left panels) The $\langle v_2^2 \rangle$, $\langle (\delta p_T)^2 \rangle$, and $\langle v_2^2 \delta p_T \rangle$ correlations calculated by HIJING (open points) compared to STAR data [38] (filled points). The HIJING subevent result are relatively 12% smaller than the full-event result for $\langle v_2^2 \rangle$, and likely similar for $\langle (\delta p_T)^2 \rangle$ and $\langle v_2^2 \delta p_T \rangle$. (Middle and right panels) Copy of part of Figure 3 from Ref. [38] with hand-drawn illustrations of how the STAR data points would move and the extracted U nucleus deformation parameters would change if non-hydrodynamic effects were corrected according to HIJING.

the nonflow V_2 . The overall effect of $\langle v_2^2 \delta p_T \rangle$ correlations in HIJING would cause a more negative U+U/Au+Au ratio of $\langle v_2^2 \delta p_T \rangle$ by approximately 16% in the top 0-5% centrality, again several times the estimated systematic uncertainty due to nonflow in [38]. This is illustrated in the center- and right-bottom panels of Fig. 4.

Note that in our simulations spherical nuclei are used for both Au and U. Deformed nuclei may enhance fluctuations in p_T and in jet production, the effects of which are likely minor. On the other hand, nuclear deformation would not generate a negative v_2 - p_T correlations in HIJING as the physics underlying those correlations are jets and resonance decays; hydrodynamic physics causing the v_2 - p_T anti-correlations is not present in HIJING. A larger v_2 - p_T correlations in U+U due to deformation would cause the nonflow correction to be even more negative for $\langle v_2^2 \delta p_T \rangle$, whereas a larger p_T fluctuations in U+U would reduce the correction for $\langle (\delta p_T)^2 \rangle$.

It is worth to emphasize that the nonflow and non-

hydrodynamic correlations in HIJING are several times the nonflow systematic uncertainties estimated in Ref. [38]. Correcting for those non-hydrodynamic correlations calculated by HIJING would result in a quadruple deformation parameter β_{2U} of the U nucleus different from that obtained by STAR, even beyond the quoted *total* uncertainty [38] (see the right panels of Fig. 4). Those total systematic uncertainties include not only those on nonflow but also all other sources such as experimental systematics from analysis cut variations and theoretical systematics from hydrodynamic model parameter dependencies [38]. We thus conclude that the extracted deformation parameter β_{2U} from relativistic heavy-ion collisions in Ref. [38] is premature.

It is noteworthy that HIJING is only one particular model in describing relativistic heavy-ion collisions, primarily for jet production and jet quenching. It is used here mainly to illustrate the potential significance of nonflow contamination; it is not meant to be *the* correction

for experimental data, so no attempt is made to assess systematic uncertainties on such a correction by HIJING. The red boxes drawn in the right panels of Fig. 4 are merely the shaded area of the STAR data shifted by the HIJING corrections, keeping the total uncertainties the same.

In real data analysis, a more thorough and rigorous study would be required to correct for nonflow contamination and assess the systematic uncertainties on such corrections, for example, by investigating not only HIJING but also other heavy-ion models and by rigorous estimation of nonflow in real data. One data-driven estimate was performed by STAR exploiting the η reflection symmetry in symmetric heavy-ion collisions; the estimated nonflow in central Au+Au collisions is on the order of 20% [35]. Another viable data-driven technique is to perform 2-dimensional $(\Delta\eta, \Delta\phi)$ fits to two-particle correlations [33, 34, 46, 47]; a recent such study indicates an approximately 40% nonflow in central isobar collisions [33, 34], in line with the central Au+Au data considering multiplicity dilution of nonflow. Assuming inverse multiplicity scaling of nonflow over the entire centrality from peripheral to central collisions, the 70-80% peripheral Au+Au measurement ($v_2^{\text{peri}} \approx 6.9\%$), if taken as all nonflow, would constitute a 30% nonflow, i.e., $(v_2^{\text{peri}})^2 \frac{N_{\text{ch}}^{\text{peri}}}{N_{\text{ch}}^{\text{cent}}}$, in the 0-5% central collision measurement ($v_2^{\text{cent}} \approx 2.4\%$) [48]. Comparing the accumulative correlations as functions of p_T in the top 0-5% central Au+Au to MB proton-proton collisions suggests a nonflow contribution on the order of 15% in the former [49]. All these estimates indicate an appreciable nonflow contribution in central Au+Au collisions.

5. CONCLUSIONS

It is well known that anisotropic flow measurements are contaminated by nonflow correlations from resonance de-

cays, jet correlations, etc. In general, non-hydrodynamic correlations can give rise to many types of correlations including p_T fluctuations and v_2 - p_T correlations. There is absolutely no question about those correlations being present and relatively large, as seen in HIJING, a non-hydrodynamic model with no flow.

In the recent preprint by STAR [38], elliptic flow v_2 , p_T fluctuations, and v_2 - p_T correlations were measured in U+U and Au+Au collisions and their ratios in the most central collisions were directly compared to hydrodynamic calculations, with minimal estimation of nonflow contamination, to extract an Uranium quadrupole deformation parameter $\beta_{2\text{U}} = 0.297 \pm 0.013$ of high significance. We examine non-hydrodynamic contributions to those correlation quantities using the HIJING model and demonstrate that those contributions could present significant contamination to the STAR measurements. Correcting for those contamination according to HIJING would yield a $\beta_{2\text{U}}$ value beyond the quoted total uncertainty. We conclude that the nonflow contamination is inadequately estimated in the STAR measurements [38] and the extracted $\beta_{2\text{U}}$ parameter is deemed premature. Additional homework is needed to put it onto a firm ground.

Our study is motivated by the recent STAR work at RHIC, but our message goes beyond. The most important message of our study is that nonflow and non-hydrodynamic correlations should be earnestly assessed with faithful systematic uncertainties assigned, either after correction wherever possible or without correction, before drawing physics conclusions from comparing experimental data to hydrodynamic calculations.

ACKNOWLEDGMENT

This work is supported in part by the U.S. Department of Energy (Grant No. DE-SC0012910).

-
- [1] Jean-Yves Ollitrault. Anisotropy as a signature of transverse collective flow. *Phys.Rev.*, D46:229–245, 1992.
 - [2] B. Alver, B.B. Back, M.D. Baker, M. Ballintijn, D.S. Barton, et al. Importance of correlations and fluctuations on the initial source eccentricity in high-energy nucleus-nucleus collisions. *Phys.Rev.*, C77:014906, 2008.
 - [3] Wei Li. Observation of a ‘Ridge’ correlation structure in high multiplicity proton-proton collisions: A brief review. *Mod.Phys.Lett.*, A27:1230018, 2012.
 - [4] James L. Nagle and William A. Zajc. Small System Collectivity in Relativistic Hadronic and Nuclear Collisions. *Ann. Rev. Nucl. Part. Sci.*, 68:211–235, 2018.
 - [5] Miklos Gyulassy and Larry McLerran. New forms of QCD matter discovered at RHIC. *Nucl.Phys.*, A750:30–63, 2005.
 - [6] Ulrich Heinz and Raimond Snellings. Collective flow and viscosity in relativistic heavy-ion collisions. *Ann.Rev.Nucl.Part.Sci.*, 63:123–151, 2013.
 - [7] Liang He, Terrence Edmonds, Zi-Wei Lin, Feng Liu, Denes Molnar, and Fuqiang Wang. Anisotropic parton escape is the dominant source of azimuthal anisotropy in transport models. *Phys. Lett.*, B753:506–510, 2016.
 - [8] Paul Romatschke. Collective flow without hydrodynamics: simulation results for relativistic ion collisions. *Eur. Phys. J.*, C75(9):429, 2015.
 - [9] Aleks Kurkela, Urs Achim Wiedemann, and Bin Wu. Opacity dependence of elliptic flow in kinetic theory. *Eur. Phys. J.*, C79(9):759, 2019.
 - [10] Aleks Kurkela, Aleksas Mazeliauskas, and Robin Törnkvist. Collective flow in single-hit QCD kinetic theory. *JHEP*, 11:216, 2021.
 - [11] Giuliano Giacalone. Observing the deformation of nuclei with relativistic nuclear collisions. arXiv:1910.04673 [nucl-th], 2019.

- [12] Giuliano Giacalone, Jianguyong Jia, and Chunjian Zhang. Impact of Nuclear Deformation on Relativistic Heavy-Ion Collisions: Assessing Consistency in Nuclear Physics across Energy Scales. *Phys. Rev. Lett.*, 127(24):242301, 2021.
- [13] Huichao Song, Steffen A. Bass, Ulrich Heinz, Tetsufumi Hirano, and Chun Shen. 200 A GeV Au+Au collisions serve a nearly perfect quark-gluon liquid. *Phys. Rev. Lett.*, 106:192301, 2011. [Erratum: *Phys. Rev. Lett.* 109,139904(2012)].
- [14] Hanlin Li, Hao-jie Xu, Ying Zhou, Xiaobao Wang, Jie Zhao, Lie-Wen Chen, and Fuqiang Wang. Probing the neutron skin with ultrarelativistic isobaric collisions. *Phys. Rev. Lett.*, 125(22):222301, 2020.
- [15] Derek Teaney. The Effects of viscosity on spectra, elliptic flow, and HBT radii. *Phys. Rev. C*, 68:034913, 2003.
- [16] Harri Niemi, Gabriel S. Denicol, Pasi Huovinen, Etele Molnar, and Dirk H. Rischke. Influence of the shear viscosity of the quark-gluon plasma on elliptic flow in ultrarelativistic heavy-ion collisions. *Phys. Rev. Lett.*, 106:212302, 2011.
- [17] Sergei A. Voloshin. Testing the chiral magnetic effect with central U+U collisions. *Phys.Rev.Lett.*, 105:172301, 2010.
- [18] D. E. Kharzeev, J. Liao, S. A. Voloshin, and G. Wang. Chiral magnetic and vortical effects in high-energy nuclear collisions—A status report. *Prog. Part. Nucl. Phys.*, 88:1–28, 2016.
- [19] Volker Koch, Soeren Schlichting, Vladimir Skokov, Paul Sorensen, Jim Thomas, Sergei Voloshin, Gang Wang, and Ho-Ung Yee. Status of the chiral magnetic effect and collisions of isobars. *Chin. Phys.*, C41(7):072001, 2017.
- [20] Jie Zhao and Fuqiang Wang. Experimental searches for the chiral magnetic effect in heavy-ion collisions. *Prog. Part. Nucl. Phys.*, 107:200–236, 2019.
- [21] Mohamed Abdallah et al. Search for the chiral magnetic effect with isobar collisions at $\sqrt{s_{NN}}=200$ GeV by the STAR Collaboration at the BNL Relativistic Heavy Ion Collider. *Phys. Rev. C*, 105(1):014901, 2022.
- [22] Hao-Jie Xu, Xiaobao Wang, Hanlin Li, Jie Zhao, Zi-Wei Lin, Caiwan Shen, and Fuqiang Wang. Importance of isobar density distributions on the chiral magnetic effect search. *Phys. Rev. Lett.*, 121(2):022301, 2018.
- [23] Hanlin Li, Hao-jie Xu, Jie Zhao, Zi-Wei Lin, Hanzhong Zhang, Xiaobao Wang, Caiwan Shen, and Fuqiang Wang. Multiphase transport model predictions of isobaric collisions with nuclear structure from density functional theory. *Phys. Rev.*, C98(5):054907, 2018.
- [24] S. Voloshin and Y. Zhang. Flow study in relativistic nuclear collisions by Fourier expansion of Azimuthal particle distributions. *Z.Phys.*, C70:665–672, 1996.
- [25] Peter Jacobs and Xin-Nian Wang. Matter in extremis: Ultrarelativistic nuclear collisions at RHIC. *Prog.Part.Nucl.Phys.*, 54:443–534, 2005.
- [26] Fuqiang Wang. Novel Phenomena in Particle Correlations in Relativistic Heavy-Ion Collisions. *Prog. Part. Nucl. Phys.*, 74:35–54, 2014.
- [27] Kevin Dusling, Wei Li, and Björn Schenke. Novel collective phenomena in high-energy proton–proton and proton–nucleus collisions. *Int. J. Mod. Phys.*, E25(01):1630002, 2016.
- [28] Nicolas Borghini, Phuong Mai Dinh, and Jean-Yves Ollitrault. Are flow measurements at SPS reliable? *Phys.Rev.*, C62:034902, 2000.
- [29] Nicolas Borghini. Momentum conservation and correlation analyses in heavy-ion collisions at ultrarelativistic energies. *Phys. Rev.*, C75:021904, 2007.
- [30] Quan Wang and Fuqiang Wang. Non-flow correlations in a cluster model. *Phys.Rev.*, C81:064905, 2010.
- [31] Jean-Yves Ollitrault, Arthur M. Poskanzer, and Sergei A. Voloshin. Effect of flow fluctuations and nonflow on elliptic flow methods. *Phys.Rev.*, C80:014904, 2009.
- [32] Arthur M. Poskanzer and S.A. Voloshin. Methods for analyzing anisotropic flow in relativistic nuclear collisions. *Phys.Rev.*, C58:1671–1678, 1998.
- [33] STAR Collaboration. Upper Limit on the Chiral Magnetic Effect in Isobar Collisions at the Relativistic Heavy-Ion Collider. arXiv:2308.16846 [nucl-ex], 2023.
- [34] STAR Collaboration. Estimate of Background Baseline and Upper Limit on the Chiral Magnetic Effect in Isobar Collisions at $\sqrt{s_{NN}} = 200$ GeV at the Relativistic Heavy-Ion Collider. arXiv:2310.13096 [nucl-ex], 2023.
- [35] N. M. Abdelwahab et al. Isolation of flow and non-flow correlations by two- and four-particle cumulant measurements of azimuthal harmonics in $\sqrt{s_{NN}} = 200$ GeV Au+Au collisions. *Phys. Lett.*, B745:40–47, 2015.
- [36] Yicheng Feng, Jie Zhao, Hanlin Li, Hao-jie Xu, and Fuqiang Wang. Two- and three-particle nonflow contributions to the chiral magnetic effect measurement by spectator and participant planes in relativistic heavy ion collisions. *Phys. Rev. C*, 105(2):024913, 2022.
- [37] Chunjian Zhang and Jianguyong Jia. Evidence of Quadrupole and Octupole Deformations in Zr96+Zr96 and Ru96+Ru96 Collisions at Ultrarelativistic Energies. *Phys. Rev. Lett.*, 128(2):022301, 2022.
- [38] STAR Collaboration. Imaging Shapes of Atomic Nuclei in High-Energy Nuclear Collisions. arXiv:2401.06625 [nucl-ex], 2024.
- [39] Xin-Nian Wang and Miklos Gyulassy. HIJING: A Monte Carlo model for multiple jet production in p p, p A and A A collisions. *Phys.Rev.*, D44:3501–3516, 1991.
- [40] Miklos Gyulassy and Xin-Nian Wang. HIJING 1.0: A Monte Carlo program for parton and particle production in high-energy hadronic and nuclear collisions. *Comput.Phys.Commun.*, 83:307, 1994.
- [41] C. Loizides, J. Nagle, and P. Steinberg. Improved version of the PHOBOS Glauber Monte Carlo. *SoftwareX*, 1-2:13–18, 2015.
- [42] B.I. Abelev et al. Systematic measurements of identified particle spectra in pp, d+Au and Au+Au collisions from STAR. *Phys.Rev.*, C79:034909, 2009.
- [43] Björn Schenke, Chun Shen, and Derek Teaney. Transverse momentum fluctuations and their correlation with elliptic flow in nuclear collision. *Phys. Rev. C*, 102(3):034905, 2020.
- [44] Bjoern Schenke, Chun Shen, and Prithwish Tribedy. Running the gamut of high energy nuclear collisions. *Phys. Rev. C*, 102(4):044905, 2020.
- [45] Govert Nijs and Wilke van der Schee. A generalized hydrodynamizing initial stage for Heavy Ion Collisions. arXiv:2304.06191 [nucl-th], 2023.
- [46] J. Adams et al. Delta phi Delta eta Correlations in Central Au+Au Collisions at $s(\text{NN})^{1/2} = 200$ -Gev. *Phys. Rev. C*, 75:034901, 2007.
- [47] G. Agakishiev et al. Anomalous centrality evolution of two-particle angular correlations from Au-Au collisions at $\sqrt{s_{NN}} = 62$ and 200 GeV. *Phys. Rev. C*, 86:064902, 2012.

- [48] J. Adams et al. Azimuthal anisotropy in Au+Au collisions at $\sqrt{s_{NN}} = 200$ -GeV. *Phys.Rev.*, C72:014904, 2005.
- [49] J. Adams et al. Azimuthal anisotropy and correlations at large transverse momenta in p+p and Au+Au collisions at $s(NN)^{1/2} = 200$ -GeV. *Phys. Rev. Lett.*, 93:252301, 2004.